

Supporting Information for

**Softening upon Adsorption in Nanoporous Materials:
a Counter-Intuitive Mechanical Response**

Félix Mouhat, David Bousquet, Anne Boutin, Lila Bouëssel du Bourg,
François-Xavier Coudert, Alain H. Fuchs

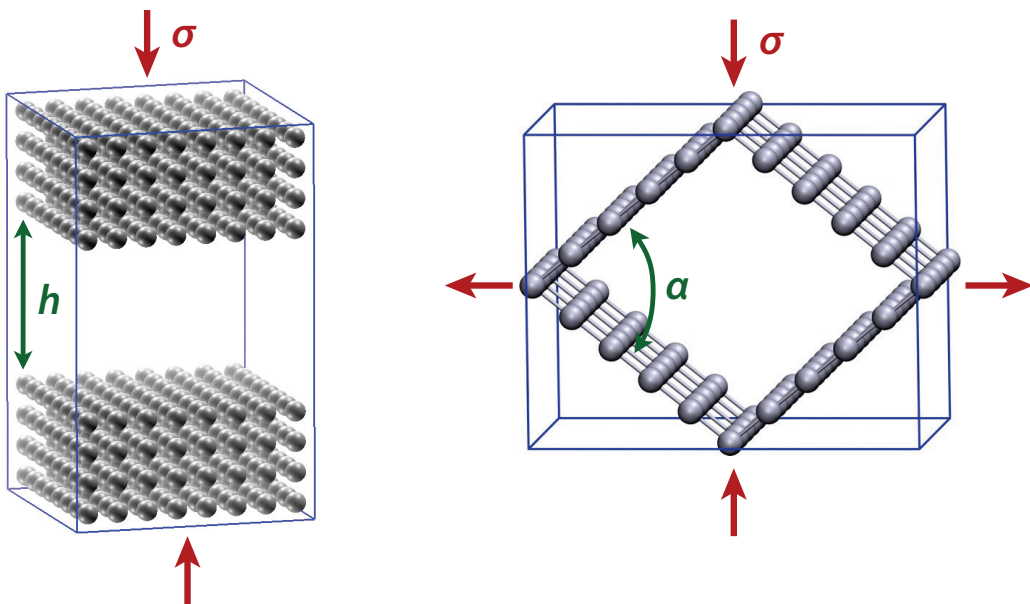


Figure S1: Depiction of the two model microporous frameworks studied in this work, showing the order parameter for the flexibility mode (in green) and associated stress (in red).

Left: the slit pore deformation is characterized by the single order parameter h (height of the slit pore), with the unit cell fixed in the other two directions. The elastic constant relevant to this deformation (and only non-infinite coefficient of the stiffness tensor) is C_{33} .

Right: the lozenge-shaped pore is a one-dimensional pore of rhombus cross-section, modelling the large-pore phase of the MIL-53 metal-organic framework. The length of the sides of the rhombus is kept fixed, and the only deformation allowed is the change in rhombus angle α . The elastic constant associated with this deformation (and only non-infinite coefficient of the stiffness tensor) is C_{66} .

System	Thermodynamic ensemble	Results
Slit pore	Osmotic ($N_{\text{host}}, \mu_{\text{ads}}, \sigma, T$)	Fig. 2, black line
Slit pore	Grand canonical ($N_{\text{host}}, \mu_{\text{ads}}, V, T$)	Fig. 2, blue line
Lozenge pore	Grand canonical ($N_{\text{host}}, \mu_{\text{ads}}, V, T$)	Fig. 3
ZIF-8	Isobaric-isothermal ($N_{\text{host}}, N_{\text{ads}}, \sigma, T$)	Text and ref. 31
ZIF <i>nog</i>	Isobaric-isothermal ($N_{\text{host}}, N_{\text{ads}}, \sigma, T$)	Fig. 4

Table S1: Summary of the molecular simulations reported in this work, and the thermodynamic ensembles used for each.

Calculation of elastic constants

From Monte Carlo simulations in the osmotic thermodynamic ensemble, where the unit cell volume V is not fixed but the mechanical stress σ is imposed, the elastic constants C_{ij} were calculated from the fluctuations of the strain of the unit cell:

$$C_{ij}^{-1} = \left(\frac{V}{k_B T} \right) (\langle \varepsilon_i \varepsilon_j \rangle - \langle \varepsilon_i \rangle \langle \varepsilon_j \rangle)$$

with ε the strain tensor, k_B is Boltzmann's constant and T is the temperature.

Molecular simulation of model pore systems

- Geometric parameters for the two model pore systems are given in Refs. 39 and 40.
- Each Monte Carlo simulation was performed for at least 10^8 steps in order to converge both the unit cell loading, cell deformation and elastic constants (the later being the longer to converge).
- Osmotic ensemble simulations were performed at ambient conditions: $T = 298$ K, and $\sigma = 1$ bar.
- Monte Carlo moves: 60% translation, 20% insertion or deletion, 20% unit cell change.
- Lennard-Jones (12–6) wall-fluid parameters: $\sigma = 3.4$ Å, $\varepsilon = 240$ K.
- Lennard-Jones (12–6) fluid-fluid parameters: $\sigma = 3.5$ Å, $\varepsilon = 250$ K.
- A cut-off radius of half the unit cell size was employed.

The relationship between the k elastic constant of the slit pore and its C_{33}^0 elastic modulus is the following, with c_0 the unit cell parameter of the relaxed pore in the z direction and V the unit cell volume:

$$k = \frac{V}{4c_0^2} C_{33}^0$$

Molecular simulation of ZIFs (ZIF-8 and nog)

Molecular dynamics (MD) simulations of the ZIFs, both empty and with CH₄ molecules loaded in their pores, were performed in the isostress-isothermal ensemble (N , σ , T) using the NAMD 2.9 software package,¹ where the source code for the barostat was patched in order to allow the unit cell to be fully flexible.² The temperature was fixed using Langevin dynamics on the heavy atoms, with a damping coefficient of 10 ps⁻¹. The pressure was fixed by a modified Nosé–Hoover method, which is a combination of the constant pressure algorithm proposed by Martyna et al.³ with piston fluctuation control implemented using Langevin dynamics.⁴ We used a piston oscillation period of 0.2 ps and a piston decay time of 0.1 ps. An integration time step of 1 fs was used, and each MD simulation was run for 5 ns, of which the first 1 ns was discarded as an equilibration period and not used for the calculation of averages and time correlations. Full three-dimensional periodic boundary conditions were employed. Electrostatic interactions were treated using the particle mesh Ewald (PME) method, and a cut-off distance of 14 Å was used for the summation of Lennard-Jones interactions. A classical force field was used to describe intra- and intermolecular interactions of the ZIF structures, as well as the ZIF/CH₄ intermolecular interactions, as described in Ref. 2.

A complete set of input files, corresponding to 9 CH₄ molecules in ZIF *nog* (as well as the NAMD 2.9 software patch), is included as Supporting Information.

Calculation of pore deformation and elastic constants through GCMC simulations

Because of the high computational cost of calculating elastic constants directly in the osmotic ensemble, we have devised a method to approximate them with series of calculations in the simpler Grand Canonical ensemble. We start by writing the derivative of the elastic constants:

$$\left(\frac{\partial C_{ij}}{\partial \mu}\right) = \frac{1}{V} \left(\frac{\partial^3 \Omega}{\partial \mu \partial \varepsilon_i \partial \varepsilon_j} \right) = -\frac{1}{V} \left(\frac{\partial^2 N_{ads}}{\partial \varepsilon_i \partial \varepsilon_j} \right) - \frac{C_{ij}}{V} \left(\frac{\partial V}{\partial \mu} \right)$$

where Ω is the osmotic thermodynamic potential. The terms on the right hand side can be evaluated from series of GCMC calculations with varying values of strain, obtaining the second derivative from finite differences. For example, in the case of the slit pore, GCMC simulations are performed at varying values of pore height h between 14 and 15 Å and a varying chemical potential μ . From these values of $(\partial C_{ij}/\partial \mu)$ and the known value at $\mu = -\infty$ (which is the elastic constant of the empty host), we can then reconstruct the evolution of C_{ij} upon adsorption, as a function of μ or N_{ads} . We can see on Figure 2 that this indirect treatment reproduces the main features of the adsorption-induced softening at intermediate loading, and stiffening at full loading.

¹ J. C. Phillips, R. Braun, W. Wang, J. Gumbart, E. Tajkhorshid, E. Villa, C. Chipot, R. D. Skeel, L. Kalé, and K. Schulten, *J. Comput. Chem.* 26, 1781 (2005)

² L. Bouëssel du Bourg, A. U. Ortiz, A. Boutin and F.-X. Coudert, *APL Mater.* 2, 124110 (2014)

³ G. J. Martyna, D. J. Tobias, and M. L. Klein, *J. Chem. Phys.* 101, 4177 (1994)

⁴ S. E. Feller, Y. Zhang, R. W. Pastor, and B. R. Brooks, *J. Chem. Phys.* 103, 4613 (1995)